We are IntechOpen, the world's leading publisher of Open Access books Built by scientists, for scientists

6,900
Open access books available

185,000
International authors and editors

200M
Downloads

Our authors are among the

154
Countries delivered to

TOP 1%
most cited scientists

12.2%
Contributors from top 500 universities



WEB OF SCIENCE™

Selection of our books indexed in the Book Citation Index in Web of Science™ Core Collection (BKCI)

Interested in publishing with us?
Contact book.department@intechopen.com

Numbers displayed above are based on latest data collected.
For more information visit www.intechopen.com



13

Fourier Transform Photocurrent Spectroscopy on Non-Crystalline Semiconductors

Jakub Holovský
Institute of Physics AS CR, v. v. i.
Czech Republic

1. Introduction

Spectroscopic methods are massively used in material physics, because as seen already from Einstein's explanation of photoeffect phenomenon material response to light is wavelength sensitive. Such sensitivity is one of key characteristics for semiconductors and therefore spectral dependence of conductivity on light excitation is of strong interest. Band structure of electron configuration in semiconductors projects into the spectra of light absorption, emission or photocurrent. In Fig. 1. such projection into spectrum of absorption coefficient (details will be explained in paragraph 4.1) can be seen. Although absorption can be measured optically, very low light absorptance cannot easily be measured so the method of measurement of photocurrent upon light illumination is used instead. Basically the aim of the photocurrent spectroscopy is to obtain the curve like the one on the right of the Fig. 1.

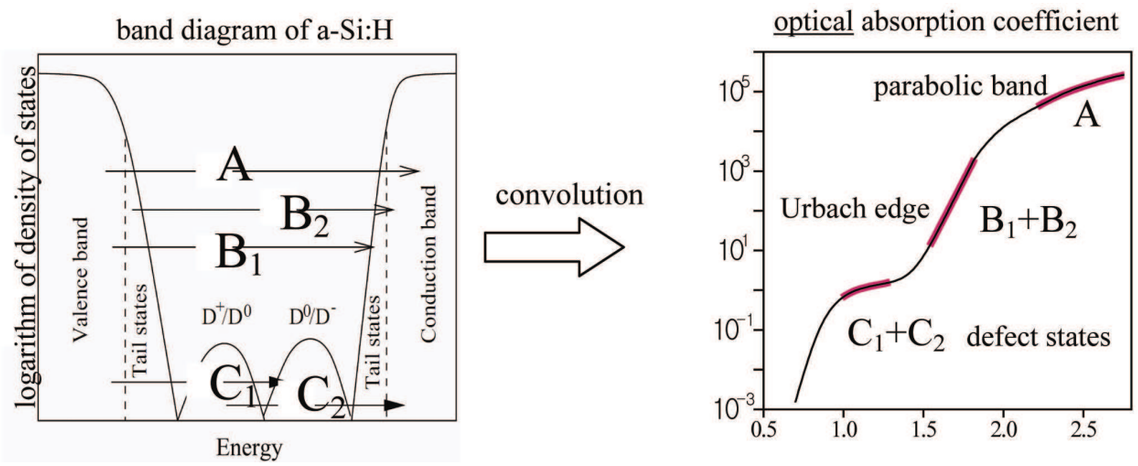


Fig. 1. On the left: band structure of density of electronic states of amorphous silicon
On the right: optical absorption coefficient curve with indicated regions attributed to different electron transitions - desired result of photocurrent spectroscopy

Photocurrent method based on the Fourier transform (F-T) and called FTPS (Fourier Transform Photocurrent Spectroscopy) is a spectroscopic method where monochromator is replaced by FTIR (Fourier Transform Infrared) spectrophotometer. This method was firstly

reported in 1997 (Tomm et al., 1997) and later (Poruba et al., 2001), (Vaněček et al., 2002) well promoted mainly for the purposes of R&D of thin film silicon photovoltaics where the quality of semiconducting layers are monitored. In earlier method CPM (Constant Photocurrent Method) keeping the photocurrent constant during the measurement by complicated modulation of light intensity was necessary (Vaněček et al., 1981). In FTPS method this condition is fulfilled automatically and also the measurement is much faster. The method can be more sensitive and more reproducible. Due to its first publications mainly on microcrystalline silicon people usually understand the FTPS simply as a method used for quality analysis of this material although its potential is not limited only to microcrystalline silicon and its use on amorphous silicon and many other non-crystalline semiconductors was successfully proven. Many practical issues of the use of FTPS are discussed in this chapter too.

In general Fourier-transform (F-T) represents in optical spectroscopy strong alternative to the classical approach based on light dispersion (monochromator). One advantage (Felgett) is that in F-T spectroscopy light of single wavelength is not isolated but only "labeled" or "encoded" so that the measurement can be performed for all wavelengths simultaneously. The spectral distribution of measured effect is obtained subsequently after mathematic decoding. Second advantage (Jacquinot) is much higher limit for resolution with the same light throughput than in monochromators. These are main reasons why F-T spectroscopy is used for example in FTIR vibrational analysis. The FTIR measurements have standardized procedures and usually not deep understanding of principles is necessary. Since FTPS is not a standard application of FTIR instrument, many other issues except the main advantages have to be considered for correct measurement and interpretation. Understanding of them is based on some fundamental principles that are in condensed form discussed in next section.

2. Principles of Fourier-transform spectroscopy

In this paragraph we want to discuss in condensed form the principal issues important for correct measurement. For F-T spectrometers many alternatives exist, but most common and instructive is the F-T spectrometer based on Michelson's interferometer, or 'modulator' as depicted in Fig. 2. Incoming light from source is partly transmitted and partly reflected by beamsplitter. Each part continues into separate delay line with mirrors at the ends. After reflection on the mirrors two beams superpose at the beamsplitter again but with mutual phase shift given by product of wavenumber[1] ν and retardation Δ, i.e. mutual path difference of the two beams. One of the mirror moves linearly with velocity u, so that retardation is time dependent: $\Delta=u(t-t_0)$. It follows from theory of light coherence that the intensity of light superposition will depend on retardation and thus will change in time t as cosine function:

$$I(\nu,t) = B(\nu)\left(1+\cos(2\pi\cdot 2\nu u(t-t_0))\right) \tag{1}$$

The factor B(ν) is baseline and represents compound spectrum of additional effects i.e.: lamp radiance, transmittance and reflectance of beamsplitter and effects of other optical elements in the instrument. Formula 1 can be regarded as 'coding key' that attributes to each wavenumber ν harmonic modulation in time with frequency f that depends linearly on the

[1] Used in infrared spectroscopy, unit is inverse centimeter cm^{-1}, $\nu(cm^{-1})=10^7/\lambda(nm)$

wavenumber according to formula 2. The modulation is for typical conditions (λ=500-1600nm, u=0.16cm/s) in the range from 2 kHz to 6 kHz. If some of the factor in the experiment exhibits frequency dependence correction to that has to be done, see paragraph 3.6.

$$f = 2\nu u \tag{2}$$

When the vavenumber is 'encoded' into modulation frequency the light beam is ready for measurement. Then other elements in the measurement should be introduced: optical filter with spectral transmittance $F(\nu)$ and detector that transforms light intensity into electrical current. Its spectral dependence can be labeled as $D(\nu)$. We make one more step and we will also go from one discrete wavenumber to continuous spectrum so that we will add the signs of integration over ν. Then we get formula 3 where the electrical current J is a function only of time t. The example of such time evolution called interferogram is in Fig. 2.

$$J(t) = J_0 + \int_{-\infty}^{\infty} D(\nu)\cdot F(\nu)\cdot B(\nu)\cdot\cos\left[2\pi\cdot 2vu(t-t_0)\right]\mathrm{d}\,\nu \tag{3}$$

It is very important that the detector is linear so that the current is a linear function of intensity and can be therefore represented in formula 3 linearly (y=D·x). Non-linear detectors (y=D·x+D´·x²+…) would introduce higher powers of cosine and would lead to parasitic contributions to the modulation at higher multiples of ν (higher harmonics) !
In formula 3 we can easily recognize Fourier-transform (for precision we renormalize time as $t'=(t-t_0)\cdot 4\pi u$), so that we can directly write bidirectional formulae between time domain and wavenumber domain (with **FT** as a symbol for Fourier transform):

$$J(t') = \sqrt{\pi/2}\cdot\mathbf{FT}\left(B(\nu)\cdot F(\nu)\cdot D(\nu)\right) \tag{4}$$

$$B(\nu)\cdot F(\nu)\cdot D(\nu) = \sqrt{2/\pi}\cdot\mathbf{FT}\left(J(t')\right) \tag{5}$$

Formula no. 5 finally gives simple instruction to calculate spectra from recorded interferogram. However only theoretically, because the interferogram is obviously not infinite in time and is sampled only in finite steps. The finite length has then effect on resolution through Rayleigh criterion: Two beams can be distinguished only if they differ in full retardation by full wavelength. Which transformed to domain of wavenumbers means that the theoretical resolution (in cm^{-1}) is inverse of max. retardation Δ_{MAX} (in cm). In reality due to the Gibbs phenomenon and often used triangular apodization[2] the theoretical limit of resolution will for given max. retardation Δ_{MAX} (Δ_{MAX} is twice the mirror path) be ~ $2/\Delta_{MAX}$, that can go well below $0.1cm^{-1}$. These issues are important in FTIR but not in FTPS (typically resolution $32cm^{-1}$ and triangular apodization is used). According to Jacquinot advantage the F-T spectrometer can have up to 100 times higher light throughput than dispersive instrument for given resolution (Griffiths 1977). In reality the built-in sources are optimized only for high resolution where the light throughput is comparable with monochromator with low required resolution (for thin film Si resolution Δν/ν or Δλ/λ around 0.01 is

[2] In F-T spectroscopy the spectra are not corrupted by convolution with instrument function but with F-T of envelope function that can be artificially reshaped by so called apodization so that the convolution has better representation of sharp features, but lower resolution.

enough) and thus lower resolution with high throughput is possible only with external light source, see paragraph 3.3.

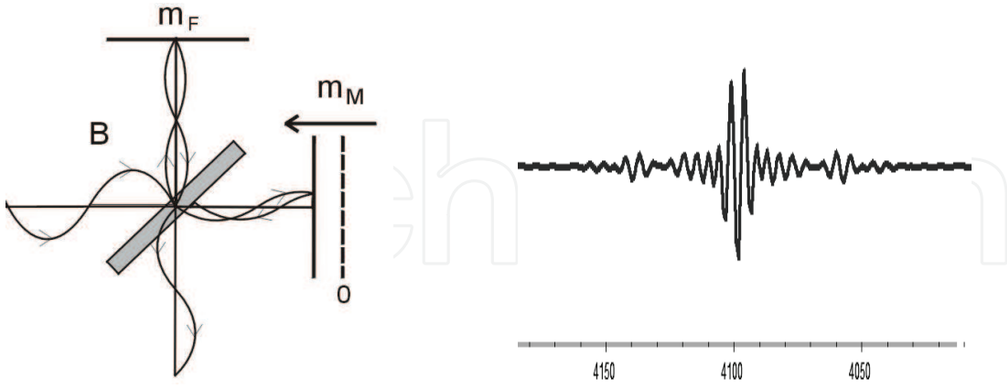


Fig. 2. On the left: Michelson's interferometer. Light enters from left side, is splitted by beamsplitter (**B**), reflected at fixed ($\mathbf{m_F}$) and movable ($\mathbf{m_M}$) mirrors and then exits downwards. On the right: Example of interferogram – amplitude of signal in domain of time/mirror position

The relation between resolution and spectral range is bidirectional and so it concerns the finite sampling density (sampling 'resolution'). Due to Nyquist-Shannon-Kotelnikov theorem that says roughly that the maximal distinguishable frequency is half of the sampling frequency, F-T spectrometer is unable to distinguish between multiples of $15798/g$ cm^{-1}, where *15798* is wavenumber of red laser and g is parameter called sample spacing[3]. This constraint unfortunately requires division of the spectrum by appropriate cut-off filters into parts from $m \cdot 15798/g$ cm^{-1} to $(m+1) \cdot 15798/g$ cm^{-1} that have to be measured separately. Fortunately modern instruments have $g=0.5$ and allow measurement up to $31600 cm^{-1}$ which with using halogen light as a source needs no filtering and spectrum can be measured at once. But for example measurement of FTPS of thin films silicon with $g=1$ and halogen source requires adding long-pass filter with edge above 633nm ('red glass').

Felgett (or multiplexing) advantage is basically the fact that we can measure all wavelengths simultaneously and thus measure much faster. It is also the reason why the FTPS can replace CPM method (see paragraph 4.5). These advantages have one important disadvantage. Like most measuring instruments F-T spectrometer has limited dynamic range, i.e. the ratio between highest and lowest values measured together and with small relative error. This is especially important in the case of steep absorption edge[4] in photocurrent measurement of semiconductors that is investigated always in logarithmic scale. The effective dynamic range is approximately 100 but can still vary a little according to the shape. In the case of slow slopes the dynamic range can be higher whereas in abrupt steep edges the dynamic range can be lower. Therefore for measurement of higher dynamic range spectra have to be measured with optical filters that reduce or eliminate strong parts of the spectra against weaker parts. Regarding the noise we can bring one argument that

[3] In FTIR the sampling is made with the help of red laser ($15798 cm^{-1}$) interference. Sample spacing expresses distance of sampling points as a fraction of distance between 2 maxima of red laser interference.

[4] Due to the Gibbs phenomenon sharp steps are not perfectly represented by truncated F-T.

also supports the Felgett advantage: Noise is proportional to the square root of spectral range, but signal as we can see from formula 3 is proportional linearly to the spectral range, so the signal to noise ratio in turn increases with spectral range (Griffiths 1977). Therefore it is better for enhancing the dynamic range to use filters that are not cut-off so they don't totally eliminate high signal region but are 'smooth' and only reduce the high signal region and maintain nonzero signal in broad region.

Summary:

- each wavelength is modulated by different frequency $f=2vu$
- resolution is limited by mirror path length and aperture dimensions and can easily go below 0.1cm^{-1}
- signal linearity is essential condition
- optical cut-offs are necessary for combination of halogen source with sample spacing greater than 0.5
- dynamic range is ~100 and has to be enhanced by additional optical filtering
- filtering by smooth filters is better than by cut-off filters

3. FTPS experiment

FTPS method is atractive due to its simple implementation to the research grade FTIR (Fourier-transform infrared) spectrometer that has option to external (e.g. photoacoustic) detector. FTIR spectrophotometers are since 1990's widely used for optical vibrational spectroscopy (range from 400 to 25000 cm^{-1}). They are user-friendly compact instruments including source, modulator and detector. Advantage is if the instrument has an availability of sample spacing 0.5. Then, only a high-quality low-noise current preamplifier (with voltage output), suitable optical filters and sample holder and cables are necessary for measurement of solar cells. For layers on glass additional voltage source has to be used.

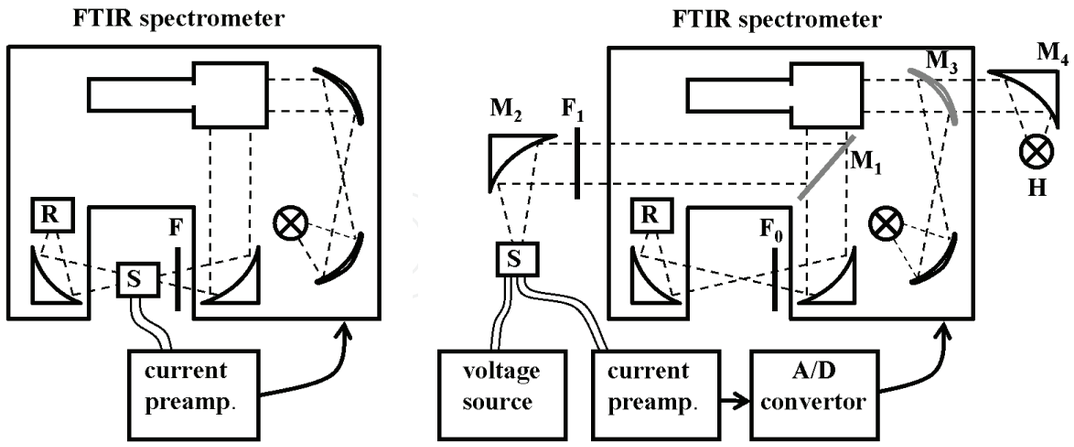


Fig. 3. On the left: 'simplest' FTPS setup where sample **S** is inside the sample area, reference **R** is measured without sample and with filter **F** (generally different for sample and reference). On the right: 'richest' FTPS setup with beam reflected out by sliding mirror $\mathbf{M_1}$ to external focusing mirror $\mathbf{M_2}$, two different positions for filter $\mathbf{F_0}$, $\mathbf{F_1}$, external source **H**, external mirror $\mathbf{M_4}$, rotating mirror $\mathbf{M_3}$, external A/D convertor and voltage source

Other components such as external focusing mirror, external A/D converter or external light source can be used optionally, see Fig. 3. Special features (not shown here) are internal motorized filter wheel and grey filter wheel. Measurement of a sample (layer on glass) in sample area has advantage of possibility of measurement of transmittance directly by internal reference detector. Measurement is performed as a sequence of inteferogram scans. The time for one scan is based on mirror velocity and max. retardation. Recorded interferograms are corrected for the phase and summed together. Signal to noise of the calculated spectrum increases with number of scans. 1 scan at velocity 0.16cm/s and resolution 32 cm^{-1} takes approx. 1 second and typically few hundreds of scans are necessary for the most 'difficult' samples. The evaluation is performed according to simple logic that is obvious from the formula 5: We compare two measurements of compound spectrum $B(\nu) \cdot F(\nu) \cdot D(\nu)$ one from sample (indexed by 1) and one from reference (indexed by 0), see Fig. 3 and formula 6. The sample and reference can play a role of any factor in the formula. In FTIR the sample (and reference) plays a role of optical filter $F(\nu)$, in FTPS the sample plays a role of detector $D(\nu)$. Baseline is for both measurement the same and its effect cancels out, as seen in formula (6). Filters can be for both measurements generally different. We correct mathematically afterwards their effects by dividing the signal by the transmittance spectrum of the filter that was used for the measurement. If we don't know the transmittances of the filters, we have to use same filters for sample as for reference which in general means a limitation.

$$D_1(\nu) = \frac{\mathbf{FT}\left(J_1(t')\right)}{\mathbf{FT}\left(J_0(t')\right)} \cdot \frac{F_0(\nu)}{F_1(\nu)} \cdot D_0(\nu) \tag{6}$$

Obviously, the response of the reference detector $D_0(\nu)$ has to be known too. Since in optics we calculate with photon fluxes rather than energy fluxes D means quantum efficiency of the photon - electron generation in the sample or detector. Absolute quantum efficiency of sample and reference detector is difficult to find out, so we always measure it relatively and additional procedures have to be used for absolute scaling, e.g. according to additional optical transmittance and reflectance measurement in medium absorption region. For the purposes of FTIR measurement, the knowledge of quantum efficiency of reference detector is not necessary and therefore it is usually unknown and for purposes of FTPS has to be found out. Typically the detectors are pyrodetectors, so they have flat response in energy flux (amperes per watt). By multiplying their response by photon energy (in electronvolts) we obtain quantum efficiency (no. of electrons per one photon). By this we obtain quantum efficiency for modulation frequencies close to zero. For obtaining quantum efficiency at real conditions of wavelength dependent modulation at 2-6 kHz frequency we could either do an approximate frequency dependence correction (paragraph 3.6) or rather do a calibration by frequency independent detector[5].

3.1 Sample preparation

Generally three types of samples can be measured: 1) Layer of semiconductor on low alkaline glass (low-cost glass will cause problems with charging of impurities) is measured

[5] Commercial calibrated c-Si detectors are unfortunately strongly frequency dependent, but can be used for low frequency calibration of e.g. thin film solar cells with low frequency dependence and these can then be used for calibration of reference detector in FTPS.

in coplanar configurations, i.e. two contacts on layer are evaporated by Al or NiCr or alternatively drawn by graphite paste. For smooth layers interdigitated contacts with thin gaps can be used, but for scattering layers spacing at least 1.5 mm is necessary (Poruba et. al 2000), details in paragraph 5.1. Voltage typically in range from 50V to 500V is applied. Light is perpendicularly focused to sample so that it has to entirely fill the gap between contacts. Sample should be illuminated from layer side, only for ideal smooth layers or for comparative measurement illumination from substrate side is possible (paragraph 4.2). Advantage of these samples is possibility of transmittance measurement (Fig. 3) at the same time and easy and accurate interpretation of the results, details in paragraph 4.2. Disadvantage is that these samples do not correspond to material grown on real substrates. 2) More close to real conditions e.g. in solar cell technology might be layers grown on conductive substrates as ZnO or SnO_2 coated glass. These have to be measured in sandwich configuration when measured semiconductor layer is sandwiched between the conductive substrate and another planar electrode deposited on top. At least one of the electrodes has to be transparent for illumination. In this case the current flows perpendicularly to surface and thus only very small distance is between the electrodes. Usually also band bending effects are presented and so small voltages (up to 2V) have to be carefully chosen to compensate such effects (Poruba et al. 2003), (Holovský et al. 2010). 3) Solar cells on the other hand don't require any preparation and typically are measured without any voltage applied (Poruba et al. 2001). Application of voltage is used to simulate real working conditions of solar cells (Bailat 2004). Monolithic multijunctions e.g. tandems or modules have to be selectively light-biased, more information in paragraph 5.3.

3.2 Choice of the FTIR instrument

The main requirements for the FTIR instrument used for FTPS are related to sample spacing, mirror velocity, beamsplitter, light source, optical windows and detector. As described above, the lowest possible sample spacing of 0.5 is strongly recommended and spacing of 1 is necessity. Lowest mirror velocity at the lowest sample spacing in true linear mode[6] should be 0.16 cm/s. FTPS measurement is in the visible and near-infrared range (0.4-2.5 μm) and so the choice of material for beamsplitter and windows is mainly quartz or sapphire, detector should be pyrodetector (e.g. thermoelectrically cooled deuterated triglycin sulphate), mirrors should be aluminum and light source should be halogen lamp. Choice of the halogen lamp is especially advantageous due to its intensity increase towards regions of low absorptance of semiconductors. Usually beamsplitter, source and detector are exchangeable so that the spectrophotometer can still be used for FTIR infrared range.

3.3 External focusing mirror, external A/D converter and external light source

The external A/D converters supplied by the same manufacturers can have better performance that the built-in A/D converters in terms of number of bits, possibility of gain ranging and signal to noise ratio that can be higher significantly. The use of external A/D converter can be for some instruments impossible for measurement in the sample area and has to be combined only with external focusing mirror. External focusing mirror is more flexible in terms of size of samples, additional light biasing etc. see Fig. 4. Also the beam can

[6] Sometimes low speed modes are not true linear scans, but in principle fast step-scan modes (for step-scan mode see paragraph 6)

be focused to smaller spot to get higher intensity. Typical focal length of internal mirror is ~15 cm with the focused beam spot size 2x8 mm².

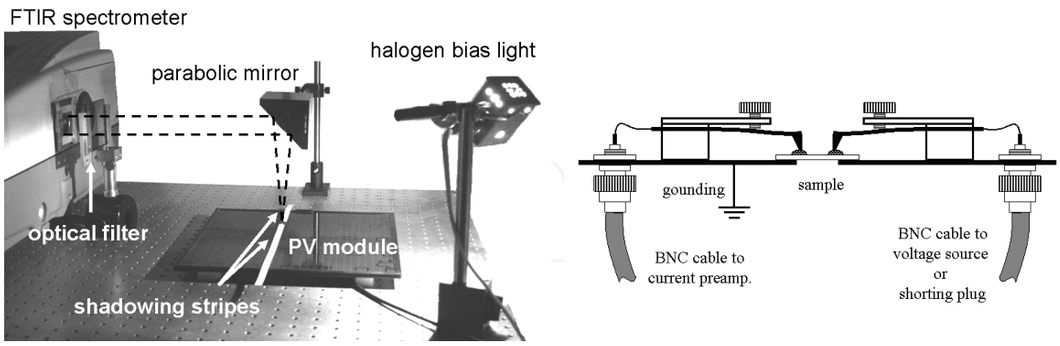


Fig. 4. On the left: FTPS setup with the use of external focusing mirror for measurement of maps of density of defects of PV modules. For selecting one spot shadowing stripes and bias light was used. On the right: sample holder for layers on glass and solar cells that have both contacts on the same side of glass substrate

The external light source can significantly increase intensity of light and also enhance its intensity in blue region. Internal halogen source has typically power of 25W, dimensions of filament approximately 2x8 mm², is intentionally kept at lower voltage and is coupled to the bench by mirror with high focal length for better resolution (~15cm). The photon flux at focus is around $2x10^{17}cm^{-2}s^{-1}$. If we use halogen lamp with 75W power with filament of comparably equal size[7] and with combination of a mirror with lower focal length (~10cm) we get approximately 7 times higher intensity. Then the resolution is no more guaranteed by automatically controlled internal aperture and has to be checked according to formula 6 where d is largest dimension of light source (or entrance slit), f is focal distance and ν_{MAX} is maximal wavenumber in the spectrum. For details see (Griffiths & de Haseth 1986).

$$\Delta\nu = (d / 2f)^2 \nu_{MAX} \tag{6}$$

For described external source and for ν_{MAX}=20000cm^{-1} resolution is $\Delta\nu$~32 cm^{-1} that is what is normally used. For maximizing intensity going to resolution $\Delta\nu$ ~100cm^{-1} is possible and intensity grows 4 times. Conservative estimate of potential intensity increase of external source is 20 times. Advantage of external source is that the FTIR instrument is more thermally stable. Disadvantage is that the bench alignment can be done only for either source, see paragraph 3.7.

3.4 Current preamplifier, voltage source and sample holder

The choice of these components will strongly affect the signal to noise ratio and thus the sensitivity and speed of the measurement. For the voltage source there is no necessity to buy expensive sources. For low voltages simple battery source is better than expensive programmable sources. For high voltages (up to 500V) some high voltage source has to be used. The important issue is the scheme of serial connection of the voltage source, sample

[7] 12V halogen lamp nominally 100W designed for vehicles from manufacturer NARVA

and current preamplifier in terms of electromagnetic noise. The use of BNC 50Ω coaxial cables has proven to be much better compared to connection by twisted pair cables. The connection in series can be easily realized by the design of a sample holder where both outer wirings are connected to metal frame and each inner wire contacts one pole of the sample, see Fig. 4. Grounding of the metal frame usually reduces noise level too. In the case of measurement without voltage source (solar cells) shorting plug is used at one of the BNC connector.

Most important is the choice of current preamplifier and state-of-the art instruments are recommended. Important parameters are: noise level, frequency cut-offs, input impedances and dynamic reserve. The noise level of preamplifier at high amplification is more critical for highly resistive samples of layers on glass (1-100GΩ). For amplification 10^7 V/A broadband noise should not be above 1 picoamper. On the other hand for measurement of solar cells and modules with generally low resisitivity (10-100Ω) dynamic reserve[8] is critical. The frequency cut-offs are inequitable in all preamplifiers at high amplifications and cause frequency dependence of signal (see paragraph 3.6) and prevent from using high amplifications. Modulation frequency range is given by formula 2 and for our spectral range and range of mirror velocities (0.16– 0.47cm/s) frequency range in low signal (=high amplification) region is 1kHz – 10kHz. High amplifications cannot be used also due to increasing input impedance. Two different preamplifiers one with lower noise level and one with higher dynamic reserve were tested on solar cell and layers on glass and it was impossible to make any unambiguous preference, see Fig. 5.

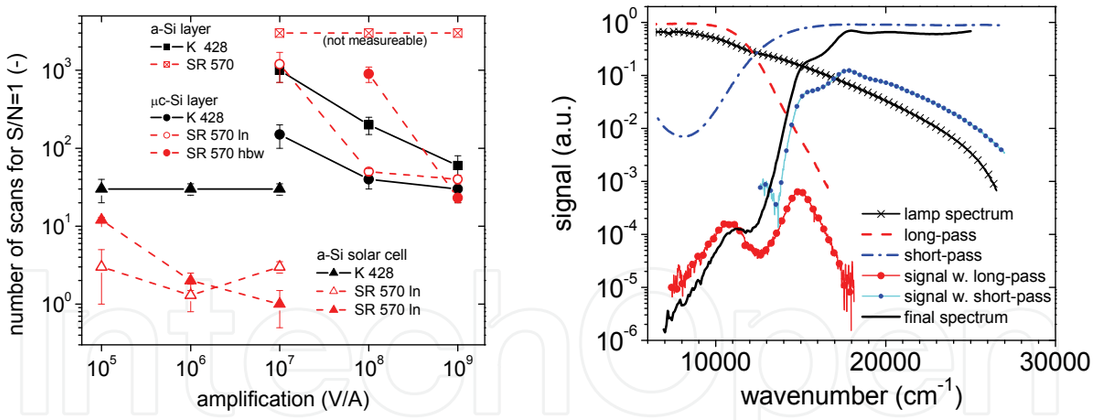


Fig. 5. Left: comparison of number of scans needed for signal to noise ratio S/N=1 for preamplifiers Standford Research 570 and KEITHLEY 428, data are based on real measurements of layers of amorphous (a-Si) and microcrystalline (μc-Si) silicon on glass and for a-Si solar cell. ('ln' = low noise mode, 'hbw'= high bandwidth mode).
Right: FTPS spectra of 250nm thick amorphous silicon measured only with 2 filters (long-pass and short-pass), transmittances of the filters and source intensity spectrum included

[8] Dynamic reserve express how larger can be broadband noise than the signal before overloading – depends on setting and location of frequency band filters

3.5 Optical filters

There are at least four reasons for using filters in FTPS: 1) Measurement with sample spacing greater than 0.5 requires using cut-off filters for both sample and reference (for details see paragraph 2). 2) Filters are necessary for improving dynamic range too. One possibility is to use cut-off filters, such as 2mm polished Si wafer for measurement of microcrystalline silicon (Poruba et al. 2002) or even set of filters for amorphous (Melskens et al. 2007) to eliminate more and more from high absorption region and to get to lower and lower absorptances. Alternative is to use less filters or even only one that only reduces light intensity at high absorption region. If the minimum of signal S that we want to measure is S_{MIN} then transmittance of ideal filter would be 1 in region where $S<100 \cdot S_{MIN}$ and $100 \cdot S_{MIN}/S$ where $S>100 \cdot S_{MIN}$ then we would measure whole curve with dynamic range only 100. For example see spectrum of long-pass filter in Fig. 5. 3) Third reason for filtering is that F-T spectroscopy doesn't reproduce spectrum where sharp step occur (absorption drop on the bandgap in amorphous Si at 1.75eV) and better results are obtained when using the filter that reduces the signal before the abrupt drop comes, see short-pass filter in Fig. 5. 4) Fourth reason for filtering is when it is necessary to keep low signal conditions. For that color or neutral density filters can be used (see section 4.5). The use of optical filters complicates strongly the automation of the FTPS because generally for different materials different filters have to be used.

3.6 Frequency dependence correction

Here we come to the main issue of FTPS. The frequency of modulation ranges from 1kHz to 10kHz and is wavenumber dependent as seen from formula 2. If performance of any part of experiment (sample, reference, preamplifier) is frequency dependent a correction for this dependence has to be done in order to obtain results same as measured at modulation frequency close to zero. Because sample and reference has different frequency dependence, formula 5 can be used only after such correction. We can suppose that the signal S at certain wavenumber ν and certain frequency f can depend on a frequency either according to formula 7 or formula 8, that means that the function Φ describing frequency dependence can be wavenumber dependent and so has wavenumber as parameter.

$$S(\nu, f(\nu)) = S(\nu, 0) \cdot \Phi(f(\nu)) \tag{7}$$

$$S(\nu, f(\nu)) = S(\nu, 0) \cdot \Phi(f(\nu), \nu) \tag{8}$$

Function Φ is unknown and can be investigated only experimentally for each sample. In FTPS the way of investigating function Φ is to make additional measurements at different velocities and observe the signal change with velocity. But because we can go from velocity 0.16 cm/s only to higher ones, function Φ can be found only around some central frequency, say 5kHz. Based on formulae 7 or 8 we can calculate signal at this frequency and so get from measured signal spectrum $S(\nu,f(\nu))$ to new spectrum $S(\nu,$ 5kHz$)$ that corresponds to spectrum as if measured at one wavelength independent frequency 5kHz. Obviously we can't get further to zero frequency. For some samples we can suppose that formula 7 holds and from it follows that $S(\nu,$ 5kHz$) = S(\nu,$ 0$) \cdot$ *constant* and so we can get correct, but relative spectrum. This explains why even for 'good' frequency dependence (formula 7) we can't measure absolutely. For high preamplification, major part of frequency dependence is caused by preamplifier for which formula 7 holds. In practice it has only sense to assume

wavelength independent frequency dependence obeying formula 7. As we will see in paragraph 4.3 and 4.6 wavelength dependence as in formula 8 can occur only for photothermal ionization effects or for samples where carrier diffusion dominates. For correction we measure spectrum at three velocities and then in set of reference wavenumber points we quantify and fit (typically by exponential) the relative decrease of signal with frequency (calculated for each point by formula 2). In next step the average of the parameter of relative decrease is made and finally one of the three curves is corrected (virtually to 5kHz). Only the curve that we want to correct (usually lowest velocity) has to be measured finely with enough scans but for the two other much less scans are necessary. Frequency dependence can be sometimes significant and can lead to shift of one end of the spectrum compared to opposite end as high as by 50%, so it is clear that the accuracy is strongly influenced by frequency dependence and so the error is usually at least few percents.

3.7 Bench alignment

For successful measurement correct bench alignment is necessary. Once properly done it does not have to be done for months. Alignment is done in commercial instruments automatically and instrument remembers alignment for each beamsplitter. It was found that the shape of a baseline spectrum depends on alignment and if bench is properly aligned the baseline (roughly spectrum of source) for quartz beamsplitter should monotonously decrease towards high wavenumbers. To do so and to enhance intensity in visible range, alignment in two steps first without filter and then with short-pass glass is necessary.

When using external source, alignement should be done as follows: 1) Make proper alignment for internal source. 2) Mark on a screen that is placed into the focus the precise position of the focal point. 3) Manually align the mirror (M_4 in Fig. 3) into axis of Michelson modulator. 4) Adjust the external source to obtain the same position and dimension of the focal point on the screen. 5) Make new alignment with external source. Then the bench will not be aligned for internal source.

Summary:

- research grade FTIR and low noise preamplifier are only necessary large investments for setting up FTPS method
- high dynamic range or low noise of the preamplifier is more important for measurement of solar cells or layers on glass, respectively
- proper choice of long-pass optical filters is main know-how in FTPS but prevents simple automation of the method
- coaxial cables and grounded sample holder is necessary for low noise signal
- frequency dependence correction is necessary for FTPS on thin film silicon
- with external source the high troughput advantage allows 20 times higher intensity
- proper two-step bench alignement is necessary for accurate measurements

4. Interpretation of FTPS

In the section 1 and Fig 1 we outlined the aim of optical spectroscopy in disordered semiconductors, e.g. amorphous silicon (a-Si) that is to get information about defect density and disorder. In section 3 we covered most of the technical issues regarding the successful measurement of a FTPS spectrum. Nice thing would be to show in this part a formula for FTPS signal as a function of defects and disorder. Unfortunately situation is much more

complex and to puzzle out its complexity a diagram (Fig. 6) is sketched where all the arrows represent one specific relation that will be discussed hereafter. In spite of the complexity of the diagram, the individual effects themselves are quite straightforward and well known in the field of semiconductors.

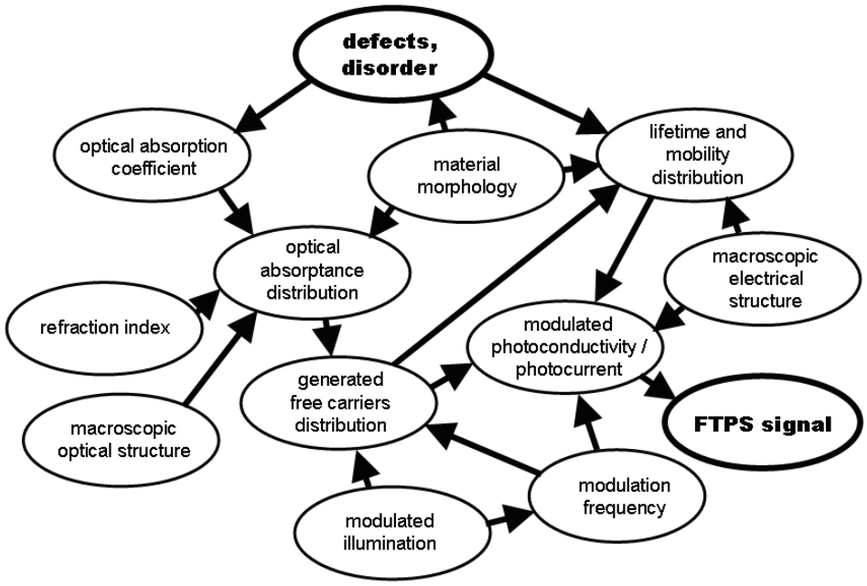


Fig. 6. Diagram shows most of the possible effects playing between defects density and disorder as input that we want to know and FTPS signal as output that we measure

4.1 From defects to absorption coefficient

Defects and disorder (their origin base on material microstructure is beyond the scope of this article) are represented as electronic states in material and characterized by spatial density and energy. In non-crystalline semiconductors these are only two parameters fully characterizing the electronic structure of material, because due to high electron scattering on irregularities no momentum quantum number and its conservation exist. So the conditions for optical excitation between occupied and unoccupied state are only energy conservation and spatial overlap of the initial and final state. Mathematically the absorption coefficient can be expressed as convolution of spatial density of occupied and unoccupied states by formula 9, where $W(\hbar w)$ is matrix element the form of which is not consensual[9].

$$\alpha(\hbar\omega) = W(\hbar\omega)\int N_V(E)\; N_C(E+\hbar\omega)\; dE \tag{9}$$

This frequently used formula holds for undoped material under low light conditions (Fermi level E_F is well defined and is close to the middle of the gap) and also low temperature limit is considered (states above E_F are unoccupied, states below E_F are all occupied).

[9] $W(E)=const$, e.g. in (Davis 1970), $W(E)= const \cdot E$, e.g. in (Jackson et al. 1985), $W(E)=const/E$, e.g. in (Vaněček et al. 1984)

material	defect energy	typ. good value	scaling constant (cm^{-2})	method	reference
a-Si	1.2 eV	<1 cm^{-1}	2.4-5x10^{16}	CPM	(Wyrsch et al. 1991)
		<2 cm^{-1}	1.2-2.5x10^{16}	PDS	
μc-Si	0.8 eV	<0.1 cm^{-1}	~ 1.7x10^{17}	CPM	(Vaněček et al. 2000)
	0.7 eV	<0.1 cm^{-1}	3.6x10^{16}	PDS	(Klein et al. 2007)

Table 1. Defect absorption energies, typical values for good quality materials and factors for recalculation into defect density (cm^{-3}) for values obtained from constant photocurrent method (CPM) and photothermal deflection spectroscopy (PDS)

In the band structure of amorphous materials the Gaussian humps in the middle represent defect states or unsaturated bonds and the tilt of the edges (band tails) represent mainly angular disorder of chemical bonds. Two vertical lines are called mobility edges, separate delocalized extended states and localized tail states and define electrical gap of the material. Y-axis in the Fig. 1 is in logarithm scale and only strong transitions are identified, i.e. only transition involving always at least one state from valence or conduction band. Transitions C_1, C_2, B_1 and B_2 project into region of subbandgap absorption on absorption coefficient. There exist more possibilities of defect density evaluation from this region (Wyrsch et al. 1991). Often used is just taking the value of absorption coefficient at some physically defined energy and multiplying it by scaling constant, see Table 1. Transition B_2 is much stronger than B_1 due to its slower slope. Exponential part of absorption coefficient is according to (Shah 2010) function of both slopes of B1 and B2, but usually is attributed only to the slope of valence band tail. For its slope the Urbach energy E_0 is defined by formula 10 (Street 1991). For good quality non-crystalline silicon material E_0 is never higher than 50 meV.

$$\alpha(\hbar\omega) = c \cdot \exp(\hbar\omega / E_0) \tag{10}$$

4.2 From structure to optical absorptance

For evaluation of optical absorptance, as seen from Fig. 6 not only absorption coefficient discussed in paragraph 4.1, but also refraction index, material and interface morphology and obviously macroscopic sample structure have to be known. Exact knowledge of all parameters and accurate calculation of absorptance for arbitrary structures is insoluble problem and therefore simple well defined samples should be measured if absolute results and not only relative comparison is desired. Simplest example is smooth weakly absorbing layer on nonabsorbing semiinfinite substrate. For the purpose of absorption coefficient measurement approximate formulae no 11, 12 and 13 presented in (Ritter & Weiser 1986) can be used:

$$A \cong \frac{(1-R_1)\left[e^{\alpha d} - 1 + R_2(1-e^{-\alpha d})\right]}{e^{\alpha d} + R_1 R_2 e^{-\alpha d} - 2\sqrt{R_1 R_2}\cos(2\gamma + \delta_1 + \delta_2)} \tag{11}$$

$$T \cong \frac{(1-R_1)(1-R_2)}{e^{\alpha d} + R_1 R_2 e^{-\alpha d} - 2\sqrt{R_1 R_2}\cos(2\gamma + \delta_1 + \delta_2)} \tag{12}$$

$$\alpha = \frac{1}{d}\ln\left(0.5\left\{ (1-R_2)(1+A/T) + \sqrt{(1-R_2)^2(1+A/T)^2 + 4R_2} \right\} \right) \tag{13}$$

Meaning of the symbols are: $r_{01} = \sqrt{R_1} \cdot \exp(i\delta_1)$, $r_{01} = \sqrt{R_1} \cdot \exp(i\delta_1)$, where r_{01}, r_{12} are Fresnell coefficients of perpendicular reflectance on first and second interface, A, T, α, d are absorptance, transmittance, absorption coefficient and thickness respectively. Formula 13 is directly derived from the two previous and contains no *cos* function and so we can profit from advantage of absence of interference patterns in ratio A/T. Therefore it is advantageous for thin films to measure absorptance and transmittance spectra simultaneously. This formula however requires absolute measurement of A and T, that is not always possible and therefore scaling according to additional optical measurement is necessary. Also knowledge of R_2 is necessary. Mathematic fit of e.g. Cauchy formula parameters of refraction index or assumption of some typical spectrum of refraction index (Vaněček 1995) is possible for calculation of R_2. The least sophisticated, but still used is to approximate the formula 11 into simple form 14 or 15. Both formulae do not take interference pattern into account and should therefore be applied to smoothened curve of A. Formula 14 is very often used and indeed by analyzing its error we can find that neglecting the term with *cos* in formula 11 and further neglecting some other terms on a way to formula 14 and attributing the result to curve with averaged interference will result in error in α of -10% in low absorption region for amorphous silicon on glass. This formula however still requires knowledge of R_1 and absolutely scaled A. Thus often R_1 is assumed to be constant and then formula 15 is used. Then only saturation value $A_{REL,MAX}$ at high absorption where $1-e^{-\alpha d} \rightarrow 1$ and thickness d have to be known. Then resulting α is correct except the region above and close to the maximum point.

$$A \cong (1-R_1)(1-e^{-\alpha d}) \tag{14}$$

$$\alpha \cong -\ln\left(1 - A_{REL} / A_{REL,MAX}\right)/d \tag{15}$$

So far theory for smooth, non scattering layer on glass was used. For measurement of samples with rough interfaces or even with bulk scattering as for example microcrystalline silicon, more complicated theory has to be used (Poruba et al. 2000). Sometimes effect of scattering can be well masked and for example accurate comparison between measurements of total and specular transmittance has to be done (Vaněček et al. 1998). Even more complicated is the evaluation of absorptance in solar cells where the transmittance of transparent conductive oxide layers (TCO) comes into play, but even here correction exists (Python 2009). Otherwise FTPS (and photocurrent in general) on real solar cells is useful mainly for comparative measurements of cells with same optical structure (TCO, roughness, back reflectors).

Presented formulae are for total absorptance, but characterizing light absorption by its total value is not always precise because absorption is generally not homogeneous due to many effects: 1) due to exponential decrease of intensity in absorbing material, 2) due to standing waves in thin films 3) due to inhomogeneity of material and thus inhomogeneity of absorption coefficient itself, 4) due to inhomogeneously distributed defects, for example close to surfaces of grain boundaries. Last two cases are not accounted in above presented calculations and so the measurement in A/T mode is not legitimate and has an effect of non-vanishing interference patterns (Vaněček et al. 1995). Moreover this effect depends on

position of highly absorbing sub-layer in the whole layer and if it is on the back side with respect to illumination, the non-vanishing interferences are not observed, inhomogeneity is masked but generally higher absorptance is observed, see Fig. 9.

4.3 From absorptance to excess carrier generation

Until now the analysis was based purely on optics. Now we want to look closely whether all absorbed photons create free charge carriers that can eventually contribute to photocurrent. In undoped amorphous silicon for example mobility of holes is much smaller and so only the transitions terminating above the conduction mobility edge can in principle contribute to photocurrent. But at room temperature the thermal excitation may release the carriers from small depth below the mobility edge above the edge and so enable them to be electrically collected. This two-step carrier generation is called photothermal ionization. The thermal ionization however has to be fast enough to be registered by phase correlated detection, because FTPS is (like other lock-in methods) based on measurement of modulated response that is correlated with excitation pulses and carriers excited too late are not accounted. In this point we get to the issue of frequency dependence dependent on wavelength (section 3.6, formula 8). Based on theory developed for Modulated Photocurrent Method (Abe et al. 1988), we can describe the effect of thermal excitation as a dispersion of the conduction mobility edge F down to energies ΔE below original mobility edge, analogical to Fermi-Dirac function as in formula 16 where symbols ω, f_0, k_B and T have meaning of modulation frequency, attempt-to-escape frequency (in a range of 10^{12} Hz), Boltzmann constant and temperature, respectively.

$$F(\Delta E) = \left[1 + \left(\frac{\omega}{f_0} \right)^2 \exp\left(\frac{2\Delta E}{k_B T} \right) \right]^{-1} \tag{16}$$

In the work of Abe the electronic states below mobility edge having overlap with F contribute as frequency dependent photocurrent signal. But not only frequency dependent signals, but also frequency independent signals from displacement current from the same electronic state are considered in his theory. So, depending on parameters in formula 16 and depending on the ratio of displacement versus real currents, different transitions will have different effect in photocurrent. In his work mainly transitions C_1 are studied at frequencies from 10Hz to 10kHz with strongest frequency dependence around 500Hz. Finally for studying the same effect directly for FTPS a comparison of photocurrent measurement by FTPS, CPM at 13Hz and DBP[10] method for wide range of frequencies was done (Holovský et al. 2008), see Fig. 8. From the comparison we see the effects of frequency dependence and displacement currents in defect region and beginning of Urbach edge in DBP at different frequencies. We also see difference between FTPS and CPM at defect reference energy 1.2 eV well below factor 2. According to previous papers (Wyrsch et al. 1991), CPM itself gives values of defect absorptance approximately twice lower than optical absorption. Similarly, our measurements systematically show difference in defect absorptance between FTPS and Photothermal Deflection Spectroscopy by factor around 2 at energy 1.2eV for amorphous silicon. It means that photocurrent generation is calculated according to same optical

[10] DBP stands for Dual Beam Photocurrent, method is explained in paragraph 4.5.

absorption coefficient as in paragraph 4.1 except the region of defect absorption where the photocurrent generation in amorphous silicon can be approximately twice lower. This principal discrepancy of different absorption coefficient for light propagation and for photocurrent generation shall not complicate our interpretation, because since the differences are in region of low homogeneous absorption ($1\text{-}exp(-\alpha d) \approx \alpha d$) we make no error by assuming light propagation according to the same absorption coefficient as corresponds to photocurrent generation. Only we have to choose correct recalculation constant in Table 1 (for FTPS same as for CPM method).

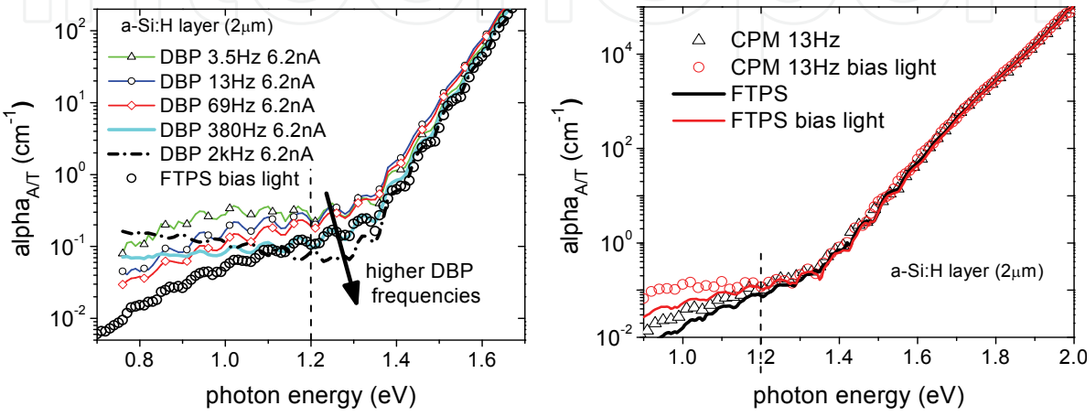


Fig. 8. Left: Dual Beam Photocurrent (DBP) spectra on 2μm amorphous Si on glass converge at higher frequencies to FTPS under bias light, at 380Hz and 2kHz DBP show anomalous deviation due to displacement currents. Right: Similar effect of light bias on FTPS and CPM methods and their comparison on the same sample

4.4 From structure to mobility lifetime distribution

When the excess carriers are generated, their efficient conduction to the collection electrodes depends on ability of the sample to conduct electrical current. As seen in Fig. 6 it depends mainly on microscopic morphology, but also presence of surfaces and so on macroscopic geometry. And also on excess carrier distribution itself, but it will be subject of next paragraph. Photocurrent in semiconductor, i.e. difference between electrical current in dark and under illumination is in simplest case given by excess carrier density n multiplied by carrier mobility μ, see equation 17. Excess carrier density is result of competition between photogeneration G described in previous paragraphs and carrier recombination that depends in simplest approximation linearly on excess carrier density. Such simple equation has steady-state solution saying that excess carrier density is a product of photogeneration G

$$j_{ph} = eE \cdot \mu \cdot n = eE \cdot G \cdot \mu \cdot \tau \tag{17}$$

and value τ called lifetime. Lifetime is a measure of recombination that in non-crystalline semiconductors is dominated by Shockley-Read-Hall recombination through active defects. Carrier mobility μ on the other hand depends on material disorder. So there are basically two material parameters that can influence conduction of generated carriers. In homogeneous samples usually also μ is homogeneous, but near surfaces τ is lower due to

surface defects. And of course in heterogeneous material both μ and τ are generally inhomogeneous.

4.5 Carrier density and lifetime

In last paragraph we defined lifetime as a value which after multiplication with generation gives excess carrier density. Now we will discuss the fact that lifetime is not a constant but a function of the excess carrier density. We discuss this phenomenon separately, because it makes the photocurrent measurement complicated. That is because activity of recombination centers is approximately given by positions of quasi-Fermi levels that depend on excess carrier density. As a consequence, conductivity on large scale is not linear with illumination, but rather sub-linear. Due to this phenomenon it is not possible to measure photocurrent for different monochromatic light of the same intensity because with different wavelength we could get photogeneration changes over many decades and so the lifetime would not be constant. On a small scale on the other hand we still assume linearity so that applying small harmonic light modulation will result in harmonic modulation of photocurrent. But for the non-linearity on the large scales there are at least three methods that solve this problem: 1) Dual Beam Photocurrent (DBP) method applies large DC light with much higher intensity than the modulated monochromatic light so that lifetime is fixed by the level on DC intensity. Drawback of this method is that, as seen in Fig. 8 the spectra still depend on level of illumination. That is due to violating the low light condition defined on the beginning in paragraph 4.1. We assume that for monochromatic light this condition is still satisfied. 2) Constant Photocurrent Method (CPM), (Vaněček 1981) adjusts the intensity of modulated monochromatic light in order to keep photocurrent constant. It will for the constant mobility mean constant excess carriers density and so constant lifetime[11]. 3) FTPS method can be regarded as combination of both CPM and DBP, because as all the wavelengths are measured simultaneously, the level of modulated photocurrent does not change and even the illumination does not change. The only question is the low light condition that would not be normally satisfied. Fortunately this condition is critical in subbandgap region only where the long-pass optical filter eliminating majority of light has to be used (paragraph 3.5).

4.6 From distributions to electrical current

We already discussed all physical properties that play role in photoconductivity: absorption coefficient, amount of absorbed light, generated excess carriers, mobility lifetime product. We already discussed their properties and mutual dependencies. In principle none of these physical values are constant and can be distributed non-uniformly. In this paragraph we should put together these distributions to get the distribution of photocurrent in our sample. So far we have not accounted for time in our thinking because all the processes we have discussed can be regarded as infinitely fast. Carrier conduction through sample is however not always so fast with respect to modulation frequency in FTPS. Treatment of such situation accurately is complicated. In simplified case of uniform doping and uniform temperature without taking into account Poisson equation we solve drift-diffusion equation 18 and continuity equation 19, where n , $\mathbf{j}$, G , τ , $\mathbf{E}$ are excess carrier concentration, current

[11] This implication may not hold only if both electrons and holes play significant role and total photocurrent is combination of both. This is not a case in non-crystalline silicon.

density, generation rate, lifetime and electric field respectively, other symbols have their usual meaning. Time enters the problem by time dependent generation *G(t)*. Solving such equations is not realistically possible and so conditions for any simplification are desirable: 1) time modulation is slow 2) lifetime is uniform in bulk, 3) absorption coefficient is uniform in bulk 4) absorption is low so that (except standing waves) the light intensity is uniform, 5) samples are thick and so without standing waves, 6) there is no additional absorption due to surface defects 7) there is no additional recombination due to surfaces.

$$\mathbf{j} = \mu \cdot \left(e\mathbf{E} \cdot n + k_B T \cdot \nabla n \right) \tag{18}$$

$$\frac{\partial n}{\partial t} = \frac{1}{e} \nabla \cdot \mathbf{j} \; + G(t) - \frac{n}{\tau} \tag{19}$$

a. If all 7 conditions are satisfied, solution of equations 18 and 19 leads to simple equation 17 and total photocurrent density is equivalent to total generation and so equivalent to total optical absorptance and according to paragraph 4.2 we can use A/T mode and formula 13. The same will practically work even if samples are thin and condition 5 is not satisfied.
b. If condition 7 is not satisfied and neither absorption is low (condition 4) we will get the situation that was for electric field applied perpendicularly to illumination described by theory of DeVore (DeVore 1956). It is the effect of signal loss at high absorption region when carriers are generated close to surface. Same theory however describes well also situation in high absorption for thin samples (when neither conditions 5 is satisfied) see Fig 9.
c. If the conditions 7 and 5 are not satisfied, and absorption is low or moderate (and not high as in previous case) the effect of standing waves with maxima close or far from surface will affect modulation of interference maxima in photocurrent. In this case the A/T mode may give some non-vanishing interference maxima in whole spectrum depending on the direction of illumination with respect to defective surface, see Fig. 9. Instead of A/T approach (formula 13) averaging of interference maxima and formula 14 should be rather used. If instead of condition 7 condition 6 is not satisfied then the effects on non-vanishing inreferences in A/T mode are observed only in low absorption regions where additional absorptance is comparable with bulk absorptance (Vaněček et al. 1995). Arguing that these two effects compensate is not very safe, because they affect different regions, see Fig. 9. In these cases the sample thickness should be chosen big enough (1 μm or more) so that the surface areas with low mobility or with additional absorption have negligible effects compared to bulk absorptance and bulk photoconductivity.
d. If one of the conditions 2 or 3 are not satisfied, for example in microcrystalline silicon, situation is overcomplicated and exotic effects can be studied e.g. by comparison of coplanar and sandwich arrangement (Unold et al. 2000) or by light biased CPM (Siebke et al. 1998).
e. Concerning the 1st condition of slow modulation, we assume that it is satisfied when $\tau << f^{-1}$ (lifetime much shorter than time period of modulation) and then $G(t) \approx G$ and thus $\partial n/\partial t \approx 0$ in equation 18. For FTPS f^{-1}=0.2ms and so for non-crystalline silicon where τ=1-10μs condition is well satisfied whereas for crystalline silicon wafers where

τ=0.1-10ms not and at least in combination with high or moderate absorption (condition 4) this leads to strong frequency dependence, and so for example using FTPS for photoelectric measurement on c-Si wafers is problematic, see Fig. 9.

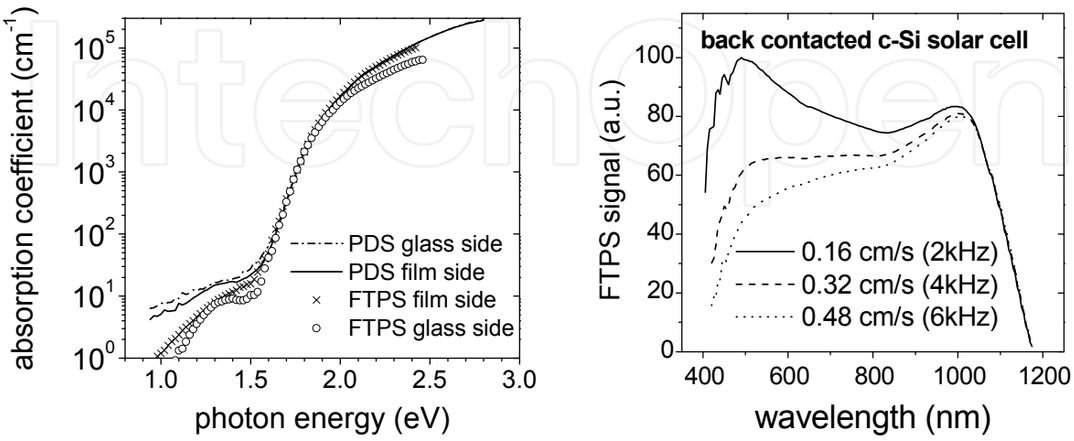


Fig. 9. Left: Result of A/T of FTPS and Photothermal deflection specroscopy (PDS) for a 350nm thick a-Si layer on glass with defective surface layer. We see non-vanishing interferences in film side measurement at low absorption in PDS and in whole range in FTPS. Deviation of PDS and FTPS in high absorption region is partly given by surface recombination. Right: Effect of high frequency modulation for c-Si solar cell observed by use of different mirror velocities

Summary:

- classical absorption coefficient in disordered materials results from convolution of density of states in low temperature limit and under dark conditions
- for optically homogeneous smooth layer A/T ratio has no interference maxima
- generation of conductive excess carriers follows optical absorption coefficient except the region far from mobility edge below the gap where its contribution is frequency dependent
- FTPS gives in defect absorption approximately twice lower value
- photocurrent depends not only on optical absorptance, but also on distribution of mobility lifetime product
- thus only for electrically (mobility, lifetime) and optically (absorption coefficient) homogeneous samples photocurrent is equivalent to optical absorptance and also A/T mode can be used
- to reduce inhomogeneity effects induced by surfaces, thicker samples (1 micrometer or more) should be used
- even for homogeneous samples measured photocurrent still depends on modulation frequency versus sample thickness and so FTPS measurement of thick samples with lifetime well above 0.2ms (c-Si wafers) can be problematic
- moreover lifetime itself is generally dependent on excess carrier density and thus 'constant photocurrent' methods like CPM or FTPS with long-pass filter are used.

5. Review of FTPS applications

Two papers give broad overview about variety of use of o FTPS: (Vaněček & Poruba 2007), (Poruba et al. 2008). In the following we will discuss separately in detail some scientific and also industrial applications.

5.1 Microcrystalline silicon

In the paragraph 4.5 we discussed the capability of use of FTPS for amorphous silicon due to its specific properties. Microcrystalline silicon is heterogeneous material with significant amorphous fraction and therefore basically same arguments can be used in case of FTPS too. Probably the first impulse was relative simplicity and good sensitivity especially on μc-Si that has advantageous shape of absorptance and with using halogen lamp as a source only one additional measurement with silicon filter is needed. The first reports of FTPS was (Poruba et al. 2001) on μc-Si p-i-n solar cells, later (Vaněček et al. 2002) on μc-Si layers on glass and later (Poruba et al. 2003) also on solar modules and layers on ZnO coated glass. As interpretation of FTPS spectra Urbach slope as a measure of disorder and absorption coefficient at energy 0.8eV as a measure of defect concentration (see Table 1) can be used. The effect of surface or bulk scattering in both p-i-n cell and layer on glass can be large and has to be corrected, see Fig.10. For layers on glass the effect depends strongly on spacing of the electrodes and minimal spacing 1.5 mm is recommended, then correction based on known surface roughness (Poruba et al. 2000) is necessary. Method of evaluation of μc-Si solar cells avoiding the effect of ZnO was well developed by Python (Python 2009). Absolute scaling can be in the case of smooth layers on glass made by approach developed for 'absolute CPM' (Vaněček et al. 1995). Without knowledge of thickness or for solar cells the approximate scaling according to crystalline silicon can be used: value at 1.35 eV is either scaled directly to value of c-Si 245cm^{-1} and we can call it normalization back to crystalline fraction (Python 2009) or is scaled to value 245cm^{-1}*Φ_c , where Φ_c is crystallinity[12]. For strong effect of scattering scaling at 1.2eV to 25cm^{-1} can be approximately done because the factor of enhancement due to light scattering changes only a little between 0.8eV and 1.2eV (Poruba et al. 2008). Broad study of microcrystalline silicon by FTPS was made at Université de Neuchâtel: (Bailat 2004), (Sculati-Meillaud 2006), (Python 2009) and correlation between FTPS and intragrain or grain boundary defects and solar cell deterioration was well verified. Microcracks in solar cells as another type of defects in solar cells are however not visible by FTPS method (Python et al. 2010).

5.2 Application of FTPS in industry at Oerlikon Solar

The power output of solar modules depends on several PECVD layers and also on several manufacturing steps before and after the PECVD deposition. To improve the module efficiency each layer and the interface between them has to be optimized. The optimization is simplified if a parameter search for each layer can be done and evaluated independently. A single layer is much faster to coat and in addition the evaluation is not affected by variations in the process steps required to manufacture a cell. The FTPS measurement is a

[12] In region around 1.35 eV α scales approximately linearly with crystallinity, however more accurate is effective medium theory (Vaněček et al. 1998) and according to (Siebke et al. 1998) scaling in broad range of crystallinity is rather exponential

relatively fast method to evaluate the defect density, which is a necessary requirement for a high quality solar cell layer.
The evaluation approach depends on the layer quality. On a coarse level poor depositions are always identified when the absorption at 0.8eV is very high e.g. above 1.0cm^{-1}. For fine tuning of already good quality layers with absorption values in the range of 0.05cm^{-1}, a comparison of only the same deposition setup and sample material is possible. Changes in the substrate e.g. with additional SnO_2 layer or different glass type leads to a change in the absorption value. This is true even if two similar glass types are compared: Schott AF32eco and Schott AF45 are coated with mc-Si in the same run, however, the FTPS data in Figure 10 shows a higher absorption for AF45 glass compared to AF32 type.

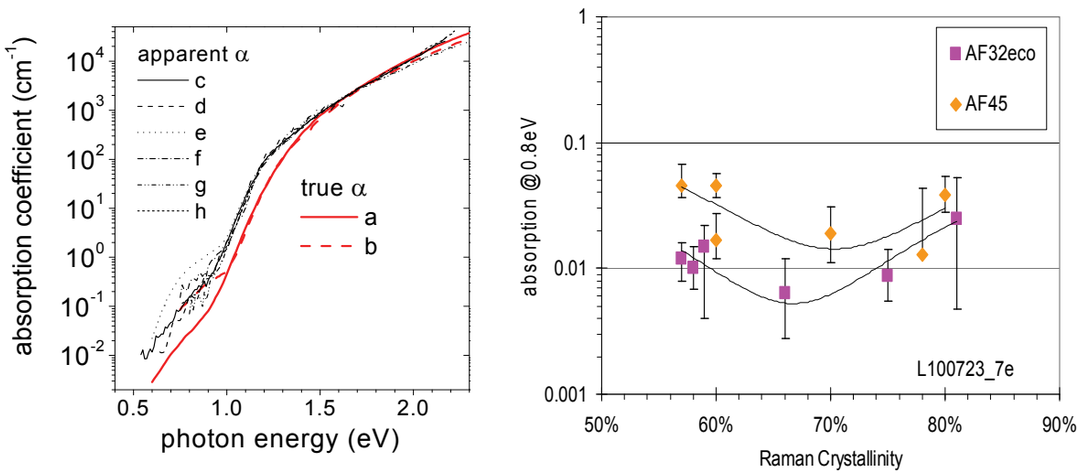


Fig. 10. Left: True absorption coefficient (a,b) and apparent absorption coefficient of 6 different materials (c-h) from different labs that all exhibit similar deviation due to the effect of scattering. Right: Effect of substrate on defect absorption for layers made in a single deposition as an example of using FTPS for module optimization in industry at Oerlikon Solar

Deposition on different substrate materials can have slightly increased absorption while still giving improved cell results. An explanation for this, is that the FTPS measurement is currently measured on AF32 glass samples placed on top off the module glass substrate. The module glass is of a different quality selected for the module requirements. The growth of the layer is affected by the different substrate surfaces. So a deposition parameter leading to a perfect layer on the Schott glass (for FTPS measurement) might lead to a non optimal layer on the large size module glass.

5.3 Amorphous silicon

FTPS on amorphous silicon is slightly more difficult than for µc-Si, because it requires different optical filters than just crystalline silicon, see Fig.5. Moreover Photothermal Deflection Spectroscopy (Jackson & Amer 1982) that is not enough sensitive for good quality µc-Si is usually enough sensitive for a-Si. The first published results of FTPS on a-Si appeared later and originated mainly from University of Delft, e.g. (Melskens et al. 2008).

Principally only FTPS can replace slower method CPM that was especially designed for amorphous silicon (paragraph 4.5) and it was shown by comparison between CPM and FTPS on a-Si (Holovský et al. 2008). FTPS was also performed on layers on a-Si codeposited on different substrates including rough conductive and non transparent Al. Special sandwich arrangement with glass covered by conductive oxide together with transparent conductive liquid (glycerol) as front contact was used. Bias voltage -1.5 V on front contact was used to create homogeneous electrical field and to compensate band bending effects. Recalculation from optical absorption to absorption coefficient was done by Monte-Carlo optical simulator, details in (Holovský et al. 2010). Measurement of multijunction solar cells monolithically interconnected was performed with the help of light biasing of the cells that are not measured, see Fig. 4. Results of such measurements can be found in (Poruba et al. 2001), (Vaněček et al. 2007) and especially in (Holovský et al. 2007) the conditions and limits of measurements tandem cells are analyzed. In tandem cells it is not possible to spatially separate the light bias or measurement beam for individual sub-cells and so the modulated generation occurs in all sub-cells. Limits of discrimination of signal from not measured cells depend on quality of diode and also on modulation frequency vs. capacity of measured cell. This unfortunately might be a problem for FTPS where high frequency modulations are used.

5.4 Nanocrystalline diamond, CIS and organic semiconductors

Together with development of FTPS on μc-Si the method was also used for measurement of subbandgap absorptance of defects and dopants of nanocrystalline diamond layers prepared by MW PECVD (Kravets et al. 2002), (Kravets 2005). Main issue in interpretation of the FTPS on nanodiamond is the effect of photothermal ionization (paragraph 4.3). This effect can be reduced by use of step-scan mode (paragraph 6) of FTIR spectrometer when ultimate sensitivity is reached with much slower speed of measurement (Remeš et al. 2007).
There has been efforts to use FTPS also for subbandgap absorption of chalcopyrite semiconductors (CIS, CIGS). FTPS spectra has been measured on solar cells only (Poruba et al. 2008), whereas measurement on layers on glass under room temperature has seemed impossible due to high dark conductivity. The Urbach slope as a measure of compositional disorder for interpretation of subbandgap region can be used (Wasim et al., 2001).
FTPS has even been used for measurement of photogeneration down to very low values in organic solar cells based on polymer-fullerene blends (Vandewal et al. 2009). Study of structural changes induced by annealing has been done (Poruba et al. 2008). According to (Vandewal et al. 2008), frequency dependence is not an issue in case of organic solar cells.

6. Discussion

In the presented text we did not pointed much to an alternative step-scan mode of FTIR. In step-scan mode the linear motion of mirror is separated into steps and in between them the mirror is stationary. Modulation is then realized by slow vibrations of the fixed mirror (phase modulation) or external chopper with lock-in amplifier (amplitude modulation). This option will certainly solve the problem of frequency dependence (paragraph 4.3), but will slow down the measurement so that the advantage compared to CPM method will be weakened. But in some cases this solution brings ultimate sensitivity that is usually not necessary e.g. for thin film silicon. Usually disadvantage of step-scan mode is sample

spacing (see paragraph 2) that is higher than 0.5. Very promising in the point of reducing modulation frequencies are new approaches based on arrays of different luminescence diodes that are used for measurement of spectra of quantum efficiency of solar cells (Young et al. 2008) or LCD-based F-T spectrophotometer (US patent no 6031609).

7. Summary

The Fourier Transform Photocurrent Spectroscopy being firstly published in 1997 has relatively short history and in this chapter we briefly reviewed its today's level of use and we more basically explained the general principles and conditions of use. Method is largely determined by the use of commercial FTIR spectrophotometer that is basis of the method. It can make the method attractive on one hand, but brings challenges on other hand. Future modern technology might show larger employment of the method. Principal advantages of F-T allow maintaining special condition of measurement such as constant photocurrent or constant illumination or allow achievement of high intensities. Method has so far been used for variety of materials: thin film silicon, nanocrystalline diamond, organic semiconductors and CIS compounds. In a laboratory FTPS can be sometimes replaced by CPM method (in most cases) or by Photothermal Deflection Spectroscopy (only non-absorbing substrates, lower sensitivity requirements) and its advantage over these methods is speed and sensitivity. Its disadvantage is wavelength dependent modulation frequency in range of kHz that requires correction procedure, complicates the interpretation of results and may even disqualify the method for specific types of materials. Despite that FTPS method has been proven to be useful in many scientific and also one industrial application.

8. Acknowledgments

The origin of this method as well as many pioneering results are mainly merits of Milan Vaněček and Aleš Poruba and many colleagues from Institute of Physics of AS CR v. v. i. The valuable feedback from solar cell industry is a merit of Stephan Jost from Oerlikon Solar, Trubbach.
This work was supported by Czech Science Foundation projects no. GA202/09/0417 and no. 202/09/H041 and 7th Framework program, project N2P, no. CP-IP-214134 and MSMT support 7E09057.

9. References

Abe, K.; Okamoto, H.; Nitta , Y.; Tsutsumi , Y.; Hattori , K. & Hamakawa, Y. (1988). Gap states in undoped amorphous silicon studied by below-gap modulated photo-current spectroscopy, *Philosophical Magazine B*, Vol. 58, No. 2, pp. 171-184 , (August 1988) ISSN: 1364-2812

Bailat, J. (2004). Growth, microstructure and electrical performances of thin film microcrystalline silicon solar cells, *PhD thesis*, Université de Neuchâtel, July 2004

Davis, E. A. (1970). Optical absorption, transport and photoconductivity in amorphous selenium. *Journal of Non-Crystalline Solids*, Vol. 4, No. C, April 1970, pp. 107-116 ISSN: 0022-3093

DeVore, H. B. (1956). Spectral distribution of photoconductivity, *Physical Review,* Vol. 102, No. 1, (April 1956) pp. 86-91

Gordijn, A.; Hoďákova, L.; Rath, J. K. & Schropp, R.E.I. (2006). Influence on cell performance of bulk defect density in microcrystalline silicon grown by VHF PECVD. *Journal of Non-Crystalline Solids*, Vol. 352 No. 9-10 (June 2006) pp. 1868–1871 ISSN: 0022-3093

Griffiths, P. R.; Sloane, H. J. & Hannah, R. W. (1977). Interferometers vs Monochromators: Separating the Optical and Digital Advantages, *Applied Spectroscopy*, Vol. 31, No. 6, (1977) pp. 485-495 ISSN: 0003-7028

Griffiths, P. R.; De Haseth, J. A. (1986). *Fourier Transform Infrared Spectrometry*, Wiley, New York

Holovský, J.; Poruba, A.; Bailat, J. & Vaněček, M. (2007). Separation of signals from amorphous and microcrystalline part of a tandem thin film silicon solar cell in Fourier transform photocurrent spectroscopy, Proceedings of *22nd EU-PVSEC*, pp. 1851-1854, ISBN: 3-936338-22-1, Milano, September 2007, WIP Munich

Holovský, J. ; Poruba, A.; Purkrt, A.; Remeš, Z. & Vaněček, M. (2008). Comparison of photocurrent spectra measured by FTPS and CPM for amorphous silicon layers and solar cells, *Journal of Non-Crystalline Solids,* Vol. 354, No. 19-25 (May 2008) pp. 2167 – 2170, ISSN: 0022-3093

Holovský, J. ; Dagkaldiran, Ü. ; Remeš, Z. ; Purkrt, A. ; Ižák, T. ; Poruba, A. & Vaněček, M. (2010). Fourier transform photocurrent measurement of thin silicon films on rough, conductive and opaque substrates, *Physica Status Solidi A,* Vol. 207, No 3, (March 2010) pp. 578-581, ISSN: 1862-6319

Jackson, W. B. & Amer, N. M. (1982). Direct measurement of gap-state absorption in hydrogenated amorphous silicon by photothermal deflection spectroscopy, *Physical Review B*, Vol. 25, No. 8 (April 1982) ISSN 1098-0121

Jackson, W. B.; Kelso, S. M.; Tsai, C. C.; Allen, J. W. & Oh, S.-J. (1985). Energy dependence of the optical matrix element in hydrogenated amorphous and crystalline silicon, *Physical Review B*, Vol. 31 No. 8 April 1985 ISSN: 1098-0121

Melskens, J.; Elzakker, G. van; Li, Y. & Zeman, M. (2008). Analysis of hydrogenated amorphous silicon thin films and solar cells by means of Fourier Transform Photocurrent Spectroscopy. *Thin Solid Films*, Vol. 516, No. 20 , (August 2008) pp. 6877–6881, ISSN: 0040-6090

Klein, S.; Finger, F.; Carius, R.; Dylla, D. & Klomfass J. (2007). Relationship between the optical absorption and the density of deep gap states in microcrystalline silicon, *Journal of Applied Physics*, Vol. 102, No. 10, p. 103501 (November 2007) ISSN: 0021-8979

Kravets, R.; Ogorodniks, V.; Poruba, A.; Moravec, P.; Nesládek, M.; Rosa, J. & Vaněček, M. (2002). Fourier-Transform Photocurrent Spectroscopy of Defects in CVD Diamond Layers. *Physica Status Solidi (a)*, Vol. 193, No. 3, (October 2002) pp. 502–507 (2002) ISSN: 1862-6319

Kravets, R. (2005). Fourier Transform Photocurrent Spectroscopy of CVD diamond, *Ph.D. Thesis*, Czech Technical University in Prague, 2005

Poruba, A.; Fejfar, A.; Remeš, Z.; Špringer, J.; Vaněček, M.; Kočka, J; Meier, J.; Torres, P. & Shah, A. (2000). Optical absorption and light scattering in microcrystalline silicon thin films and solar cells, *Journal of Applied Physiscs*, Vol. 88, No. 1, pp. 148-160 (July 2000) ISSN: 0021-8979

Poruba A.; Vaněček, M.; Rosa, J.; Feitknecht, L.; Wyrsch, N.; Meier, J.; Shah, A.; Repmann T. & Rech B. (2001). Fourier Transform Photocurrent Spectroscopy in thin film silicon solar cells, *Proceeding of 17th European Photovoltaic Solar Energy Conference*, pp. 2981-2984, ISBN: 3-936338-08-6, Munich, October 2001, WIP Munich

Poruba, A.; Špringer,J.; Mullerová, L.; Vaněček, M.; Repmann, T.; Rech, B.; Kuendig, J.; Wyrsch, N. & Shah, A. (2003). Fast and sensitive defect characterization and spectral response measurement of thin film silicon solar structures. *Proceeding of 3rd World Conference on Photovoltaic Energy Conversion (WCPEC3)*, p. 5P-A9-07, ISBN: 4-9901816-3-8, Grand Cube, Osaka, May 2003, WCPEC, Osaka

Poruba, A.; Holovský, J.; Purkrt, A. & Vaněček, M. (2008). Advanced optical characterization of disordered semiconductors by Fourier transform photocurrent spectroscopy, *Journal of Non-Crystalline Solids*, Vol. 354, No. 19-25 (May 2008) pp. 2421-2425, ISSN: 0022-3093

Python, M. (2009). Microcrystalline silicon solar cells: growth and defects, *PhD thesis*, Institut de Microtechnique, Université de Neuchâtel, March 2009

Python, M.; Dominé, D.; Söderström, T.; Meillaud, F. & Ballif, C. (2010) Microcrystalline silicon solar cells: effect of substrate temperature on cracks and their role in post-oxidation *Progress in Photovoltaics: Research and Applications*, Vol. 18, No. 7, November 2010, pp. 491–499 ISSN: 1099-159X

Remeš, Z,; Nesládek, M.; Bergonzo, P.; Barjon J. & Jomard. F (2007). Amplitude modulated step scan Fourier transform photocurrent spectroscopy of partly compensated B-doped CVD diamond thin films *Phisica status solidi (a)* Vol. 204, No. 9, pp. 2950–2956 (September 2007), ISSN: 1862-6319

Sculati-Meillaud, F. (2006). Microcrystalline silicon solar cells: theory, diagnosis and stability, *PhD thesis*, Institut de Microtechnique, Université de Neuchâtel, July 2006

Shah, A. (2010) *Thin-film silicon solar cells,* EPFL Press, ISBN 978-2-940222-36-0, Switzerland

Siebke, F. Yata, S. Hishikawa, Y. Tanaka, M. (1998). Correlation between structure and optoelectronic properties of undoped microcrystalline silicon, *Journal of Non-Crystalline Solids* Vol. 227–230 No. 2 (May 1998) pp. 977–981, ISSN: 0022-3093

Street, R. A. (1991). *Hydrogenated amorphous silicon,* Cambridge University Press, ISBN: 0 521 37156 2, Cambridge

Tomm, J. W.; Jaeger, A.; Bärwolff, A.; Elsaesser, T.; Gerhardt, A. & Donecker, J. (1997). Aging properties of high power laser diode arrays analyzed by Fourier-transform photocurrent measurements. *Applied Physics Letters,* Vol. 71, No. 16 (August 1997) pp. 2233-2235 ISSN 0003-6951

Unold, T.; Brüggemann, R.; Kleider, J.P. & Longeaud, C. (2000) Anisotropy in the transport of microcrystalline silicon, *Journal of Non-Crystalline Solids,* Vol. 266-269, No. 1 (May 2000) pp. 325-330, ISSN: 0022-3093

Vaněček, M.; Kočka, J.; Stuchlík, J. & Tříska, A. (1981). Direct measurement of the gap states and band tail absorption by constant photocurrent method in amorphous silicon, *Solid State Communications*, Vol. 39, No. 11, September 1981, pp. 1199-1202, ISSN: 0038-1098

Vaněček M.; Abrahám, A.; Štika, O.; Stuchlík, J. & Kočka J. (1984). Gap States Density in a-Si:H Deduced from Subgap Optical Absorption Measurement on Schottky Solar Cells, *Physica Status Solidi (a)* Vol. 83, No. 2 p. 617-623 (June 1984) ISSN: 1862-6319

Vaněček, M.; Kočka, J.; Poruba, A. & Fejfar, A. (1995). Direct measurement of the deep defect density in thin amorphous silicon films with the "absolute" constant photocurrent method. *Journal of Applied Physics*, Vol. 78, No. 10, (November 1995) pp. 6203-6210 ISSN: 0021-8979

Vaněček, M.; Poruba, A.; Remeš, Z.; Beck, N. & Nesládek, M. (1998). Optical properties of microcrystalline materials, *Journal of Non-Crystalline Solids* Vol. 227-230, Part 2 (May 1998) pp. 967–972 , ISSN: 0022-3093

Vaněček, M.; Poruba, A.; Remeš, Z.; Rosa, J.; Kamba, S.; Vorlíček, V.; Meier, J. & Shah, A; (2000). Electron spin resonance and optical characterization of defects in microcrystalline silicon, *Journal of Non-Crystalline Solids* Vol. 266-269, No. pp. 519-523 (May 2000), ISSN: 0022-3093

Vaněček, M. & Poruba, A. (2002). Fourier-transform photocurrent spectroscopy of micro-crystalline silicon for solar cells. *Applied Physics Letters,* Vol. 80, No. 5, (February 2002) pp. 719-721 , ISSN 0003-6951

Vaněček, M.; Kravets, R.; Poruba, A.; Rosa, J.; Nesládek, M. & Koizumi, S. (2003). Fourier transform photocurrent spectroscopy of dopants and defects in CVD diamond. *Diamond and Related Materials*, Vol. 12, No. 3-7, (March-July 2003), pp. 521-525, ISSN: 0925-9635

Vandewal, K.; Goris, L.; Haeldermans, I.; Nesládek, M.; Haenen, K.; Wagner, P. & Manca, J. V. (2008) Fourier-Transform Photocurrent Spectroscopy for a fast and highly sensitive spectral characterization of organic and hybrid solar cells, *Thin Solid Films* Vol. 516, No. 20 (August 2008) pp. 7135–7138 ISSN: 0040-6090

Vandewal, K.; Tvingstedt, K.; Gadisa, A.; Inganäs, O. & Manca, J. V. (2009) On the origin of the open-circuit voltage of polymer–fullerene solar cells *Nature Materials*, Vol. 8 No.11, pp. 904 - 909 (November 2009) ISSN: 1476-1122

Wasim, S. M.; Rincón, C.; Marín, G.; Bocaranda, P. & Hernández, E. (2001). Effect of structural disorder on the Urbach energy in Cu ternaries. *Physical Review B*, Vol. 64, No. 19, 195101 (October 2001) ISSN 1098-0121

Wyrsch, N.; Finger, F.; McMahon, T. J. & Vaněček, M. (1991). How to reach more precise interpretation of subgap absorption spectra in terms of deep defect density in a-Si:H *Journal of Non-Crystalline Solids* Vol. 137-138 Part 1 pp. 347-350 (1991) ISSN: 0022-3093

Young, D.L.; Pinegar, S.; Stradins, P. & Egaas, B. (2008) New Real-Time Quantum Efficiency Measurement System *Proceedings of the 33rd IEEE Photovoltaic Specialists Conference*, San Diego, California May 11–16, 2008 Conference Paper NREL/CP-520-42509



Fourier Transforms - New Analytical Approaches and FTIR Strategies

Edited by Prof. Goran Nikolic

ISBN 978-953-307-232-6
Hard cover, 520 pages
Publisher InTech
Published online 01, April, 2011
Published in print edition April, 2011

New analytical strategies and techniques are necessary to meet requirements of modern technologies and new materials. In this sense, this book provides a thorough review of current analytical approaches, industrial practices, and strategies in Fourier transform application.

How to reference

In order to correctly reference this scholarly work, feel free to copy and paste the following:

Jakub Holovsky (2011). Fourier Transform Photocurrent Spectroscopy on Non-Crystalline Semiconductors, Fourier Transforms - New Analytical Approaches and FTIR Strategies, Prof. Goran Nikolic (Ed.), ISBN: 978-953-307-232-6, InTech, Available from: http://www.intechopen.com/books/fourier-transforms-new-analytical-approaches-and-ftir-strategies/fourier-transform-photocurrent-spectroscopy-on-non-crystalline-semiconductors

INTECH
open science | open minds

InTech Europe
University Campus STeP Ri
Slavka Krautzeka 83/A
51000 Rijeka, Croatia
Phone: +385 (51) 770 447
Fax: +385 (51) 686 166
www.intechopen.com

InTech China
Unit 405, Office Block, Hotel Equatorial Shanghai
No.65, Yan An Road (West), Shanghai, 200040, China
中国上海市延安西路65号上海国际贵都大饭店办公楼405单元
Phone: +86-21-62489820
Fax: +86-21-62489821

© 2011 The Author(s). Licensee IntechOpen. This chapter is distributed under the terms of the Creative Commons Attribution-NonCommercial-ShareAlike-3.0 License, which permits use, distribution and reproduction for non-commercial purposes, provided the original is properly cited and derivative works building on this content are distributed under the same license.

IntechOpen

IntechOpen